Adaptive targeting of chaos

S. Boccaletti, [1,2] A. Farini, [1] E. J. Kostelich, [3] and F. T. Arecchi [1,2]

[1]*Istituto Nazionale di Ottica, I50125 Florence, Italy*
[2]*Department of Physics, University of Florence, I50125 Florence, Italy*
[3]*Department of Mathematics, Arizona State University, Tempe, Arizona 85287*

We report two adaptive methods for directing chaotic trajectories to desired targets that require only a single ''probing'' of the target by the unperturbed dynamics. In contrast to previous targeting algorithms, these methods do not require *a priori* information about the stable and unstable manifolds associated with the target point and are not restricted to invertible mappings. The methods apply small perturbations to the state variables (as opposed to parameters) and can reduce the waiting time for the system to visit the target by more than two orders of magnitude. Their robustness and lack of stringent requirements should make these methods easily implementable in experimental applications. [S1063-651X(97)50305-9]

PACS number(s): 05.45.+b

The targeting of chaos refers to a process wherein small, judiciously chosen perturbations are applied to a chaotic dynamical system to steer the orbit of a given point on a chaotic attractor to a neighborhood of some prespecified point (target) on the attractor within a specific time (usually called the target time). In many cases, a small neighborhood of a given attractor point may be visited infrequently; thus, the unperturbed dynamics may take a long time to approach a given target. Efficient targeting methods can reduce the waiting time by orders of magnitude [1–5].

A natural application of targeting is to the so-called control of chaos, which tries to maintain a chaotic trajectory in the neighborhood of a saddle periodic point. However, typical control algorithms (see, e.g., [6]) use a linearization of the dynamics that is valid only in a rather small neighborhood of the desired saddle point.

Shinbrot *et al.* [1] suggested a method for directing trajectories to targets that used the exponential sensitivity of a chaotic process to tiny perturbations of an accessible control parameter. The method has been applied to one-dimensional maps both theoretically [2] and experimentally [3] and has been extended to three-dimensional chaotic flows [4]. Kostelich *et al.* [5] suggested a targeting procedure for cases where there is more than one positive Lyapunov exponent associated with typical orbits on the attractor. (See also [7] for a review of these procedures.)

The basic algorithm in [5] consists of finding two successive changes of a single control parameter (or one change of two control parameters) to move the image of the starting point onto the stable manifold of the target. The method is robust against the presence of a small amount of noise or a small modeling error, and further developments have pointed out how it helps in switching between controlled unstable periodic orbits in higher-dimensional chaotic systems [8].

The procedure, however, has two main limitations: (1) it is only applicable to invertible mappings, and (2) it needs full *a priori* information on the stable and unstable manifolds of the target point. The latter requirement is a problem when the target is rarely visited by the natural evolution of the system, because the algorithm requires a long data acquisition time to obtain points whose orbits visit neighborhoods of the target.

A method has recently been proposed [9] to increase the number of visits to a neighborhood of an arbitrary point on a chaotic attractor by making small perturbations of the state variables of the system. This method also requires a long data acquisition time, and although it does not require an invertible map, it guarantees control only for relatively large perturbations.

In this paper, we present two adaptive strategies for targeting of chaos that overcome the difficulties mentioned above. In particular, the strategies do not require *a priori* information about the stable and unstable manifolds associated with the target point, they are not restricted to invertible mappings, and they use only small perturbations of available state variables to direct trajectories to a small neighborhood of the target. The strategies are based on a recently introduced algorithm for chaos recognition [10], control [11], and synchronization [12] that has also been utilized for filtering noise from chaotic data [13].

Let us consider a chaotic process ruled by (dot denotes temporal derivative)

$$\dot{\mathbf{x}} = \mathbf{f}(\mathbf{x}, \mu), \tag{1}$$

where $\mathbf{x}$ is a D-dimensional vector ($D \geq 3$), $\mathbf{f}$ is a nonlinear function of $\mathbf{x}$, and μ is a vector of parameters. The targeting procedure consists of two parts: (1) an algorithm that slaves the chaotic dynamics $\mathbf{x}(t)$ to a given goal dynamics $\mathbf{g}(t)$ using only small perturbations of the state variables, and (2) a goal dynamics $\mathbf{g}_T(t)$ that is compatible with the natural evolution of the system and that brings the trajectory to a small neighborhood of the target within the desired target time starting from a given initial condition $\mathbf{g}_T(0) = \mathbf{g}_0$. (The point $\mathbf{g}_0$ lies on the attractor, and typically its neighborhood is visited frequently by the unperturbed dynamics.)

The idea of slaving the state variables to a goal dynamics was first applied by Huebler for chaos control [14].

Although we assume that the dynamics are governed by Eq. (1), we emphasize that our approach does not require explicit knowledge of the vector field $\mathbf{f}$. (In contrast, the targeting methods described in [5] and [14] assume that $\mathbf{f}$ is known.) Moreover, we will show that our approach is effec-

tive when perturbations can be applied only to a single state variable in the system, whereas in the case of Ref. [14], perturbation of all state variables was needed to assure convergence of **x** to **g**.

We consider the following cases in turn: (1) the system allows detection and perturbation of all its state variables; and (2) only a single state variable is available for observation. In both cases, the algorithm can guarantee fast convergence to a neighborhood of the target.

Let us start with case (1), where one can observe and perturb all the system state variables. Let $t_{n+1} = t_n + \tau_n$, where τ_n is the adaptive observation time interval (OTI), specified below. For the ith component of **x** ($1 \leq i \leq D$), one measures the differences between the actual and the goal dynamics, given by

$$\delta x_i(t_{n+1}) = x_i(t_{n+1}) - g_i(t_{n+1}),$$

and their variation rates over τ_n, given by

$$\lambda_i(t_{n+1}) = (1/\tau_n) \log |\delta x_i(t_{n+1})/\delta x_i(t_n)|. \quad (2)$$

The successive OTI is $\tau_{n+1} = \min_{1 \leq i \leq D} \tau_{n+1}^{(i)}$, where

$$\tau_{n+1}^{(i)} = \tau_n^{(i)}[1 - \tanh(\sigma \lambda_i(t_{n+1}))]. \quad (3)$$

The next observation is performed at $t_{n+2} = t_{n+1} + \tau_{n+1}$.

The hyperbolic tangent function maps the whole range of $\sigma\lambda$ into the interval $(-1,1)$. The constant σ, strictly positive, adjusts the sensitivity of the algorithm, and it is selected to prevent τ_{n+1} from going to zero [10]. Starting at time t_0 with $\tau_0^{(i)} = \tau^{(i)}(t_0)$ and a given $\delta x_i(t_0)$, the observer produces an OTI sequence that minimizes the second variations between the actual and the goal dynamics.

The perturbation consists of the vector $\mathbf{U}(t) \equiv (U_1, U_2, \ldots, U_D)$ given by

$$U_i(t_{n+1}) = \frac{K_i}{\tau_{n+1}}[g_i(t_{n+1}) - x_i(t_{n+1})], \quad K_i > 0, \quad 1 \leq i \leq D, \quad (4)$$

to be added to Eq. (1), which now becomes $\dot{\mathbf{x}} = \mathbf{f}(\mathbf{x}, \mu) + \mathbf{U}(t)$. The vector **U** is the product of two factors: the weighting factor K_i/τ_{n+1}, which is updated by the iterative algorithm discussed above, and the difference between actual and goal dynamics, which assures the convergence to the desired behavior (indeed, this term vanishes only when actual and goal dynamics coincide).

The quantities λ_i defined in Eq. (2) give a local measure of the rate at which the actual orbit separates from the desired one. Indeed, if $\lambda_i < 0$, then locally the ith component of the trajectory approaches the goal dynamics, that is, the ith component shadows the desired dynamics. If $\lambda_i > 0$, then the ith component of the trajectory moves away from the desired one. Thus, the quantity τ reflects the frequency with which the system must be perturbed to constrain it to shadow the goal dynamics.

The algorithm provides an adaptive time scale within which the dynamics selects the correction term to be added to the evolution equation of the system. The perturbation **U** is inversely proportional to the adaptive OTI and thus is weighted by the information extracted from the dynamics

itself. As discussed in [11,12], this adaptive time scale is smaller than the time scale of the unstable periodic orbits embedded within the chaotic attractor.

Notice that in the limit $\sigma \to 0$, the algorithm becomes equivalent to Pyragas' control strategy [15], which has been successfully tested in low- and high-dimensional chaotic systems. Nonzero values of σ introduce a variable weighting factor in Eq. (4) that keeps the perturbation small and applies it only when necessary.

Let us discuss the problem of constructing the goal dynamics $\mathbf{g}_T(t)$ from a preliminary observation of the unperturbed behavior of the system. For the sake of example, we consider the three-dimensional Rössler system [16]

$$\dot{x} = -z - y$$

$$\dot{y} = x + ay \quad (5)$$

$$\dot{z} = b + z(x - c),$$

with $a = b = 0.2$ and $c = 5.7$. We first construct a partition of the phase space in parallelograms of sides $\boldsymbol{\epsilon} \equiv (\epsilon_1, \epsilon_2, \epsilon_3)$. We define $I(x_0, y_0, z_0, \boldsymbol{\epsilon}) = \{(x, y, z) : x_0 < x < x_0 + \epsilon_1, \ y_0 < y < y_0 + \epsilon_2, \ \text{and} \ z_0 < z < z_0 + \epsilon_3\}$. The initial condition $x(0) = y(0) = 1$, $z(0) = 4$ is attracted to a chaotic set, a portion of which is contained in the parallelogram $I_T(4.655\,146, -6.691\,886, 0.013\,528, \boldsymbol{\epsilon})$, where $\boldsymbol{\epsilon} \equiv (0.205\,382, 0.186\,303, 0.228\,361)$. This choice of $\boldsymbol{\epsilon}$ corresponds to a box whose sides are 10^{-2} as long as the corresponding sides of the smallest parallelogram containing the attractor for $t > 9743.658\,203$ ($t = t_T = 9743.658\,203$ is the time at which the unperturbed trajectory generated by the above initial conditions first enters I_T).

The construction of the goal dynamics exploits the natural evolution of the system from the initial condition up to the first visit to the target. We do this by constructing a web of paths, each of which is compatible with the unperturbed dynamics and connects different parallelograms to I_T. That is, we follow one or more trajectories for a given observation interval. Let $P(I_T)$ denote a preimage of I_T. We record the portions of the observed trajectories that lie in I_T and $P(I_T)$. We then determine successive preimages of $P(I_T)$, which, in most cases, have been visited previously by the portions of the observed trajectories. Going backward in time, we are able to select from the observations a path that starts from the most frequently visited parallelogram I_F and leads to the box I_T containing the target. (Once the trajectory enters I_T, which typically is near a saddle periodic orbit, we apply one of the usual control algorithms to keep the trajectory near the saddle.) The web of paths is illustrated schematically in Fig. 1. This construction requires only a single probing of the target.

The goal dynamics is an observed path from I_F to I_T. Since the natural measure of I_F is large (that is, it is frequently visited by the unperturbed dynamics), the target can be reached quickly regardless of the initial conditions.

Figure 2(a) reports the results of this targeting procedure. In the trials reported here, I_F is reached by the unperturbed dynamics for the first time when $t = 30.9$ sec, and then I_T is reached by the perturbed dynamics only 1.6 sec later. Thus, the total time required to reach the I_T is 32.5 sec, compared
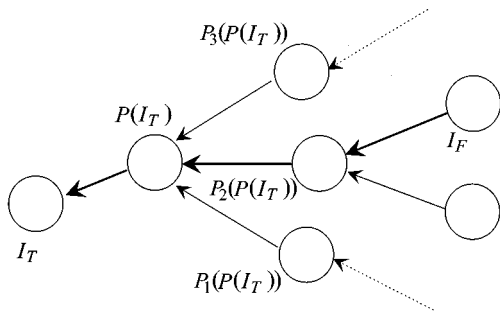
FIG. 1. Procedure for the construction of the goal dynamics $\mathbf{g}(t)$. Each bubble represents the neighborhood of a point in the phase space. I_T: target; $P(I_T)$: unique preimage of the target; $P_j(P(I_T)), j=1,2,3$: multiple preimages of $P(I_T)$; I_F: most frequently visited neighborhood. The selected path is shown as a thick line.

to 9743 sec for the unperturbed dynamics to enter the same neighborhood, for a total speedup of two orders of magnitude. Figure 2(b) illustrates the mechanism that leads the system to the target: the path that is followed by the targeting algorithm moves from high probability sections of the attractor toward lower probability sections of the same attractor, eventually reaching the desired target.

This procedure, however, requires all state variables to be accessible for measurement and perturbation. Thus it cannot be applied in experimental situations, where often only a single state variable of the system is accessible. We now show how to reformulate the adaptive targeting strategy by restricting our measurements only to the x variable of the Rössler system and applying the feedback perturbation only on the first of Eqs. (5).

It has been shown [11] that the control procedure defined by Eqs. (2)–(4) is effective in low- and high-dimensional cases even if the perturbations are restricted to a single state variable. Thus we can restrict attention to the case $i=1$.

The problem is to retrieve a suitable scalar goal dynamics $g(t)$ from the observations that is compatible with the unperturbed evolution of the system and comes at least once within a suitable neighborhood of the target. We will use the time delay embedding method [17], which allows us to reconstruct the attractor from a time series of measurements of a single variable, say $x(t)$, from Eqs. (5). By selecting a suitable delay time $\widetilde{\tau}$, we consider the D-dimensional

embedding space containing the vectors $\mathbf{x}(t)$ $\equiv[x(t),x(t-\widetilde{\tau}), \ldots, x(t-(D-1)\widetilde{\tau})]$. ($D=3$ in our case.) The reconstructed attractor retains the basic metric properties of the original; that is, points that are neighbors in the original phase space with respect to a given metric M_R remain neighbors in the embedding space with respect to some new metric M_E [18].

We let $\widetilde{\tau}=5.711\,57$; this value corresponds to the inverse frequency of the largest peak in the power spectrum of the signal $x(t)$. The target point in the original phase space, as discussed in the first example, corresponds to the point $\mathbf{x}_T$ $=(x_T(t_T),x_T(t_T-\widetilde{\tau}),x_T(t_T-2\widetilde{\tau}))=(4.727\,415,\ 4.295\,067,$ $4.929\,038)$, where t_T is the time at which the unperturbed trajectory first enters the neighborhood of the target. The idea is to retrieve a scalar goal dynamics $g(t)$ such that $g(t_0)=x_T(t_T-2\widetilde{\tau})$, $g(t_0+\widetilde{\tau})=x_T(t_T-\widetilde{\tau})$, and $g(t_0+2\widetilde{\tau})$ $=x_T(t_T)$. Here t_0 is the instant at which the unperturbed dynamics $x(t)$ first satisfies the relations $x_T(t_T-2\widetilde{\tau})-\epsilon_1/2<x(t)<x_T(t_T-2\widetilde{\tau})+\epsilon_1/2$, where $\epsilon_1=0.205\,382$. These requirements assure that the perturbations move a trajectory to the target within a target time $t_0+2\widetilde{\tau}$, starting from any initial condition.

The simplest choice of g is the recorded unperturbed evolution of x from $t_T-2\widetilde{\tau}$ to t_T. It is possible that such a choice of g is not optimal. Indeed, since our observations and perturbations are limited to a one-dimensional subspace of the original phase space, there is no certainty that at $t=t_0$ [the instant at which the variable x first enters the ϵ_1 interval of $x_T(t_T-2\widetilde{\tau})$], the other unobserved variables are within a sufficiently small distance from their values at $t_T-2\widetilde{\tau}$. The process could result in an unacceptably large initial perturbation, so that another choice of g would be necessary. Of course, other choices of g are possible. For instance, the evolution of $x(t)$ could be exploited more thoroughly by constructing two successive webs of one-dimensional paths, the first connecting $x_T(t_T-2\widetilde{\tau})$ to $x_T(t_T-\widetilde{\tau})$, and the second connecting $x_T(t_T-\widetilde{\tau})$ to $x_T(t_T)$.

The selection of a goal dynamics is complicated by the requirement that paths reach from a given point to another given point within a specified time. This requirement motivates our choice of the delay time $\widetilde{\tau}$ as the reciprocal of the frequency of the main peak of the signal power spectrum; this time is equivalent to the return time of the system onto
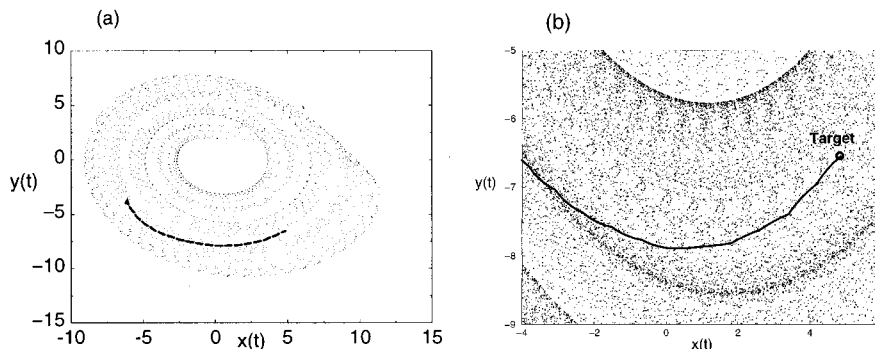
FIG. 2. (a) An (x,y) projection of the unperturbed Rössler dynamics (dots) and path followed by the perturbed dynamics to reach the target (thick dashed line). The path is inside the chaotic attractor. (b) Enlargement of (a): the path (solid line) moves from high probability regions of the attractor toward lower probability regions, until reaching I_T (indicated as Target in the Figure). Initial conditions and control parameters as in the text. $\sigma=10^{-5}$, $K_1=K_2=K_3=0.01$. Similar results hold for different choices of K_j, $j=1,2,3$, and σ due to the adaptive nature of the algorithm.
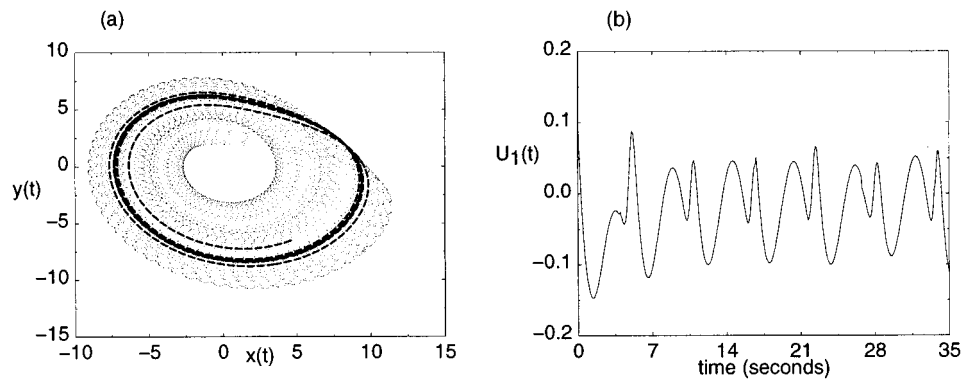
FIG. 3. (a) An (x,y) projection of the unperturbed Rössler dynamics (dots) and path followed by the perturbed dynamics to reach the target (thick dashed line). In this case the perturbation acts only on the x variable of Eqs. (5). Again, the path is inside the chaotic attractor; thus it is compatible with the natural evolution of the system and it goes from higher to lower probability regions. (b) Temporal evolution of the perturbation during the targeting process. The range spanned by U_1 is less than 1% of the range spanned by the x dynamics. Initial conditions and parameters as in the caption of Fig. 2; $K_1 = 0.02$.

its Poincaré section. Indeed, if the system is chaotic and the observation interval of the recorded unperturbed dynamics is sufficiently long, then only this choice of $\widetilde{\tau}$ assures an ergodic covering of all the states and guarantees the existence of at least one path from any initial state to any other final state within observation interval.

However, these concerns are largely obviated by a suitable choice of $\sigma \neq 0$ in the control algorithm. The adaptive nature of the procedure assures that the corrections remain small, thus allowing simpler choices of the goal dynamics.

In our case, it is sufficient to choose $g(t)$ as the unperturbed dynamics from $t_T - N\widetilde{\tau}$ to t_T ($N > 2$) to guarantee fast convergence to the target even for small perturbations. While the integer N should be selected as small as possible to minimize the waiting time, larger values of N improve the robustness of the method. Figure 3(a) reports the new phase space results for $N = 6$. The system has been left unperturbed from $t = 0$ (the same initial conditions as before) until $t = t_0 = 12.9$. Here t_0 is the instant at which the unperturbed dynamics first enters the ϵ_1 interval containing $x(t_T - 6\widetilde{\tau})$. The adaptive scalar perturbation has assured a convergence

to the target within a target time of $t_0 + 6\widetilde{\tau}$, which again is more than two orders of magnitude smaller than t_T.

The reconstruction in the real space represents a stringent test, since it demonstrates the accuracy and robustness of our method in targeting the desired I_T, even with the simplest choice of g. Figure 3(b) shows the range of fluctuations of the perturbation, and Fig. 3(a) shows the range spanned by the unperturbed x dynamics. These results illustrate the smallness of the perturbation required by the adaptive method.

It is relevant to notice that our adaptive approach accounts also for the presence of noise, as already explicitly calculated in several situations in Refs. [10–13].

In conclusion, we have presented two adaptive targeting procedures that require only a single probing of the target by the natural evolution of the system. The methods are not limited to invertible mappings and do not need *a priori* information on the stability properties of the target.

[1] T. Shinbrot *et al.*, Phys. Rev. Lett. **65**, 3215 (1990).
[2] T. Shinbrot *et al.*, Phys. Rev. A **45**, 4165 (1992).
[3] T. Shinbrot *et al.*, Phys. Rev. Lett. **68**, 2863 (1992).
[4] T. Shinbrot *et al.*, Phys. Lett. A **169**, 349 (1992).
[5] E.J. Kostelich *et al.*, Phys. Rev. E **47**, 305 (1993).
[6] E. Ott *et al.*, Phys. Rev. Lett. **64**, 1196 (1990).
[7] T. Shinbrot *et al.*, Nature (London) **363**, 411 (1993).
[8] E. Barreto *et al.*, Phys. Rev. E **51**, 4169 (1995).
[9] D. Gligorosky *et al.*, Phys. Rev. E **51**, 1690 (1995).
[10] F.T. Arecchi *et al.*, Europhys. Lett. **26**, 327 (1994).
[11] S. Boccaletti and F.T. Arecchi, Europhys. Lett. **31**, 127 (1995);
Physica D **96**, 9 (1996).
[12] S. Boccaletti *et al.*, Phys. Rev. E **55**, 4979 (1997).
[13] S. Boccaletti *et al.*, Phys. Rev. E **55**, 5393 (1997).
[14] B.B. Plapp and A.W. Huebler, Phys. Rev. Lett. **65**, 2302 (1990); E. A. Jackson and A.W. Huebler, Physica D **44**, 407 (1990).
[15] K. Pyragas, Phys. Lett. A **170**, 421 (1992).
[16] O.E. Rössler, Phys. Lett. A **57**, 397 (1976).
[17] F. Takens, in *Detecting Strange Attractors in Turbulence*, Vol. 898 of *Lecture Notes in Mathematics* (Springer-Verlag, Berlin, 1981).
[18] In most cases, and also in ours, M_R and M_E both coincide with the metric defining the Euclidean distance between points.